THE USE OF A UNIFORM EXTRAPOLATING MESH IN THE GENERAL FINITE ELEMENT METHOD

Adriano Scremin
Universidade Federal do Paraná - Departamento de Engenharia Mecânica - Curitiba - PR - Brasil - 81531-970
adriano.scremin@ufpr.br

Waldyr de Lima e Silva Jr.
Universidade Federal do Paraná - Departamento de Engenharia Mecânica - Curitiba - PR - Brasil - 81531-970
waldyr@demec.ufpr.br

Abstract. *The Generalized Finite Element Method (GFEM) is a direct extension of the standard FEM, which makes possible the accurate solution of engineering problems in complex domains where might be practically impossible to solve using standard FEM. In agreement with some aspects of the GFEM, the FEM is applied here using a topologically uniform extrapolating mesh of bilinear square elements. In this way, it is possible to generate a mesh with low computational cost and with good topological features, mainly the aspect ratio. Due to the extrapolating nature of the mesh, boundary conditions are applied through Lagrange multipliers. Practical investigations of this new approach are made in steady heat conduction for two-dimensional problems. A simple numerical quadrature for the elements crossing the boundary is used. A special investigation of the effects of the mesh orientation relative to the domain is carried out.*

Keywords*. generalized finite element method, meshless methods, Lagrange multipliers, two-dimensional Poisson problems, partition of unit method.*

1. Introduction

When dealing with Finite Element Method (FEM) one frequently spends much time on meshing. This is so because it needs a compromise between fitting the mesh to the boundary and maintaining the aspect ratio of each element during mesh generation. Depending on the domain geometry the amount of time spent increases considerably –for instance, a body with a great number of cavities- and even for a dedicated code for this task it is almost impossible to obtain a topologically well-conditioned mesh.

Bearing this in mind, approximated methods to solve boundary value problems without meshing have been recently developed (Duarte, 1995). Special examples of such approach are the Element Free Galerkin Method (EFGM) (Belytschko, 1994) and the hp-Cloud Method (hpCM) (Duarte, 1995; Duarte and Oden, 1995 and Duarte, 1996). Both adjust a base of polynomials at a set of points sprinkled over the domain minimizing the error on a weighted norm centered at these points. The resulting functions have spherical supports covering the domain in a suitable manner, as shown in Fig. (1). While the former employs directly these shape functions so obtained, the latter enriches them with a base of polynomials or others special functions in a hierarchical way. Although they do not use a mesh, they do utilize a grid for performing the integrations associated to the variational form of the original differential equations.

The base of functions of the EFGM and of the hpCM forms a partition of unity that allows easy enrichment through multiplication of any shape function by special ones more suitable for the particular problem being solved. This specific property of a partition of unity originated the so-called Partition of Unity Method (PUM) which can be seen as a generalization of the EFGM, of the hpCM and even of the FEM. The Finite Element Method, seen as a partition of unity, led to the Generalized Finite Element Method (GFEM). The formalism of the GFEM was proposed by Oden et all (1998) almost simultaneously to Melenk and Babuska (1996) proposition of the Partition of Unity Finite Element Method (PUFEM). Few years later, Sukumar et all (2000) presented the Extended Finite Element Method (X-FEM). The three methods are essentially the same except for few practical aspects. For instance, Oden et all (1998) emphasized the *hp* enrichment of the base functions, while Melenk and Babuska (1996) stressed the possibility of incorporating special base functions as a mean to achieve superior rates of convergence in problems where the solution is ‘rough’, i.e., it is not square integrable or its square integral is large. Although these new approaches use meshes as standard FEM, they do not require the same mesh quality due to their enrichment capacity.

Beyond the enrichment of the finite element shape functions, the GFEM allows to extend the covering support concept of the EFGM and of the hpCM to the finite elements. Consequently, it is possible to build a finite element mesh covering the domain that does not need to be deformed to fit the boundary. This aspect was not emphasized in the articles mentioned in the last paragraph. Although not extensively, Strouboulis et all (2001) investigated it, and they did not register experiments on the influence of the relative orientation of the mesh to the domain.

In this paper, the FEM with covering mesh is implemented in a two-dimensional Poisson problem with mixed boundary conditions, Dirichlet and Neumann, imposed through the Lagrange multipliers technique. In order to guarantee the aspect ratio control of the elements and to reduce the time spent on calculating the matrix coefficients, it is proposed a regular mesh of square elements, as shown in Fig. (2). The quadratures are performed in two manners depending on the relative position of the element to the boundary. Figure (3) illustrates them clearly: *(a)* analytically at those elements completely inside the domain; *(b)* numerically at those elements that intercept the boundary. To simplify the integrations at the latter elements, the contour line is assumed to form a straight polygon so to divide the intersection region between the element and the domain into triangles where Gauss quadrature is performed.

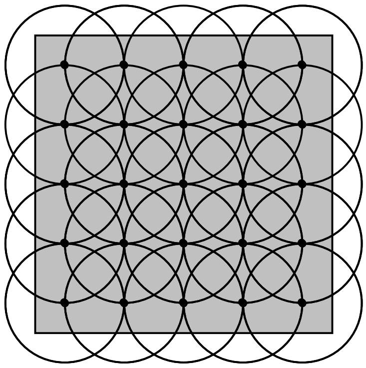

Figure 1. An example of the spherical supports covering the domain used in the EFGM and in the hpCM.

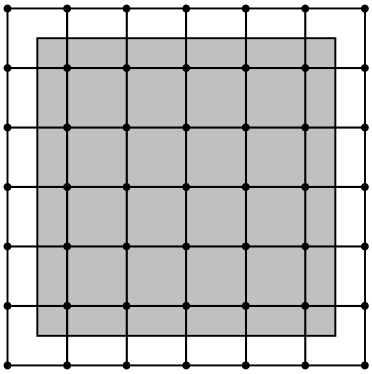

Figure 2. A regular mesh of square elements covering the domain.

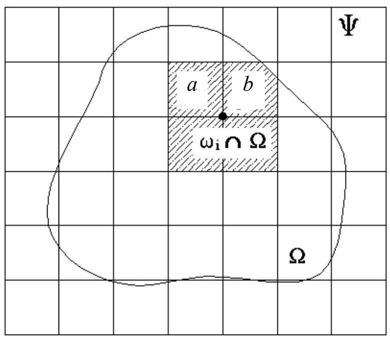

Figure 3. *(a)* elements completely inside the domain; *(b)* elements intercepting the contour boundary.

In what follows, the basic variational formulation of the Poisson problem with boundary conditions imposed through Lagrange multipliers, the numerical results for a specific problem of heat conduction, a discussion and suggestions for future researches are presented.

2. Variational formulation

Consider the two-dimensional heat conduction problem with heat generation Q governed by the Poisson equation:

$$k\nabla^2\theta + Q = 0 \tag{1}$$

in Ω, submitted to a temperature distribution on Γ_d:

$$\theta = \bar{\theta} \tag{2}$$

and to the heat flow on Γ_n:

$$q_n = \bar{q} \tag{3}$$

As the finite element covering mesh does not fit the domain contour, the boundary conditions are imposed through Lagrange multipliers. So, the functional to find a saddle point is the following:

$$\Pi(\theta, \lambda) = \frac{1}{2}\int_\Omega k\nabla\theta \cdot \nabla\theta d\Omega - \int_\Omega Q\theta d\Omega + \int_{\Gamma_n} \bar{q}\theta d\Gamma + \int_{\Gamma_d} \lambda(\theta - \bar{\theta}) d\Gamma\,, \tag{4}$$

where λ is the Lagrange multiplier.

Imposing stationarity to the functional, Eq. (4), gives:

$$\int_\Omega k\nabla\theta \cdot \nabla\delta\theta d\Omega - \int_\Omega Q\delta\theta d\Omega + \int_{\Gamma_n} \bar{q}\delta\theta d\Gamma + \int_{\Gamma_d} \lambda\delta\theta d\Gamma = 0 \tag{5}$$

$$\int_{\Gamma_d} (\theta - \bar{\theta})\delta\lambda d\Gamma = 0\,. \tag{6}$$

Let the temperature θ and the Lagrange multiplier λ be approximated respectively by:

$$\theta = \sum_i N_i \theta_i = \mathbf{N}^\mathbf{T}\mathbf{\Theta}\,, \tag{7}$$

$$\lambda = \sum_i N_i \lambda_i = \mathbf{N}^\mathbf{T}\mathbf{\Lambda}\,, \tag{8}$$

where N_i, θ_i and λ_i are respectively the finite element function, the nodal temperature and the nodal Lagrange multiplier associated to the i node. Bold symbols are used to represent matrices and vectors.

Now assuming the variations $\delta\theta$ and $\delta\lambda$ as N_i, and substituting them into Eqs. (5) and (6) results:

$$\left(\int_\Omega \nabla N_i k \nabla \mathbf{N}^\mathbf{T} d\Omega\right)\mathbf{\Theta} + \left(\int_{\Gamma_d} N_i \mathbf{N}^\mathbf{T} d\Gamma\right)\mathbf{\Lambda} - \int_\Omega N_i Q d\Omega + \int_{\Gamma_n} N_i \bar{q} d\Gamma = 0 \tag{9}$$

$$\left(\int_{\Gamma_d} N_i \mathbf{N}^\mathbf{T} d\Gamma\right)\mathbf{\Theta} - \int_{\Gamma_d} N_i \bar{\theta} d\Gamma = 0\,, \tag{10}$$

or in matrix form:

$$\begin{bmatrix} \mathbf{H} & \mathbf{C} \\ \mathbf{C}^\mathbf{T} & \mathbf{0} \end{bmatrix} \begin{Bmatrix} \mathbf{\Theta} \\ \mathbf{\Lambda} \end{Bmatrix} = \begin{Bmatrix} \hat{\mathbf{Q}} \\ \hat{\mathbf{\Theta}} \end{Bmatrix}, \tag{11}$$

where:

$$\mathbf{H} = k\int_\Omega \nabla\mathbf{N} \cdot \nabla\mathbf{N}^\mathbf{T} d\Omega\,, \tag{12}$$

$$\mathbf{C} = \int_{\Gamma_d} \mathbf{N}\mathbf{N}^\mathbf{T} d\Gamma\,, \tag{13}$$

$$\hat{\mathbf{Q}} = \int_\Omega Q\mathbf{N} d\Omega - \int_{\Gamma_n} \bar{q}\mathbf{N} d\Gamma\,, \tag{14}$$

$$\hat{\mathbf{\Theta}} = \int_{\Gamma_d} \bar{\theta}\mathbf{N} d\Gamma\,. \tag{15}$$

3. Integration on the elements

As pointed out before, when performing the integrations on each element one should consider its position relative to the boundary. If the element is completely inside, Fig. 3 *(a)*, the integrations can be easily performed analytically, and in this case, those coefficients corresponding to Eq. (12) are independent of the element size h, while the others given by Eqs. (13)-(15) are just simple functions of h.

Care must be taken when dealing with the elements intercepting the contour, Fig. 3 *(b)*. The interception region where integration should be performed in each element forms a polygon. If it is assumed for the sake of simplicity that the line corresponding to the contour is straight, this polygon can be divided into triangles where simple Gauss quadrature is performed. Exact values for the integrals can then be achieved if the order of the Gauss quadrature is chosen accordingly to that of the polynomials employed in the shape functions.

In the present article, the numerical results are obtained with this assumption. In order to avoid the error caused by this integration approach when investigating the error due to h-refinement, the covering mesh is applied to a problem with square domain.

4. Numerical results

Once the basic system of algebraic equations is posed, a numerical experiment is proposed to investigate uniform h-refinement and mesh orientation. The heat transfer problem chosen is a square of thermal conductivity 54 W/mK generating heat at rates of 54 kW/m^3, bounded by two opposite insulated walls and the others submitted to different temperatures, as shown in Fig. (4). In this case the heat flow is one-dimensional, and the analytical solution is given by:

$$\theta = -500\left(\left(x-x_0\right)\cos\alpha + \left(y-y_0\right)\sin\alpha\right)^2 + 600\left(\left(x-x_0\right)\cos\alpha + \left(y-y_0\right)\sin\alpha\right) + 273\,, \tag{16}$$

in the coordinates system (x,y). Here α designates the orientation angle of the square relative to the mesh.

All numerical experiments are carried out with regular covering meshes with bilinear square elements, as also shown in Fig. (4).

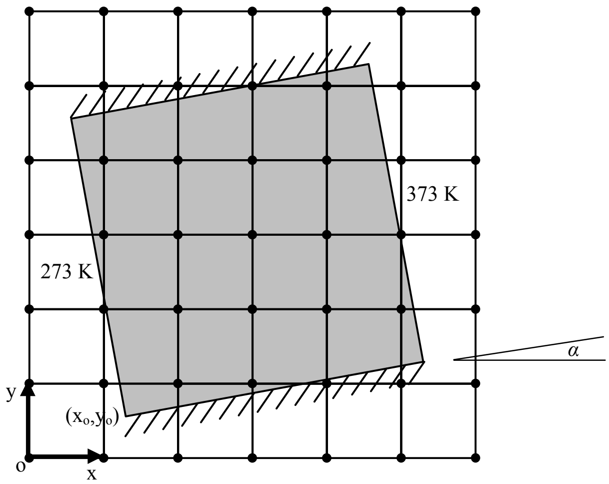

Figure 4. Square submitted to a temperature gradient: the mesh is oriented accordingly to the coordinate system (x,y).

4.1. *h*-refinement

The influence of refinement of mesh on the relative error is now investigated. In this analysis the relative orientation of the mesh to the square is given by $\alpha = 0^{o}$, 15^{o}, 30^{o} and 45^{o}. For each α the element size h is ranged from 0.5 to 0.03125 in a sequence that it is successively halved. Figure (5) shows the relative error in the H_0-norm[1], and Fig. (6) in the H_1-norm, versus the parameter h. Figure (7) shows the relative error in the H_0-norm, and Fig. (8) in the H_1-norm, versus the number of degrees of freedom (NDOF).

[1] H_m represents the Hilbert space of m order.

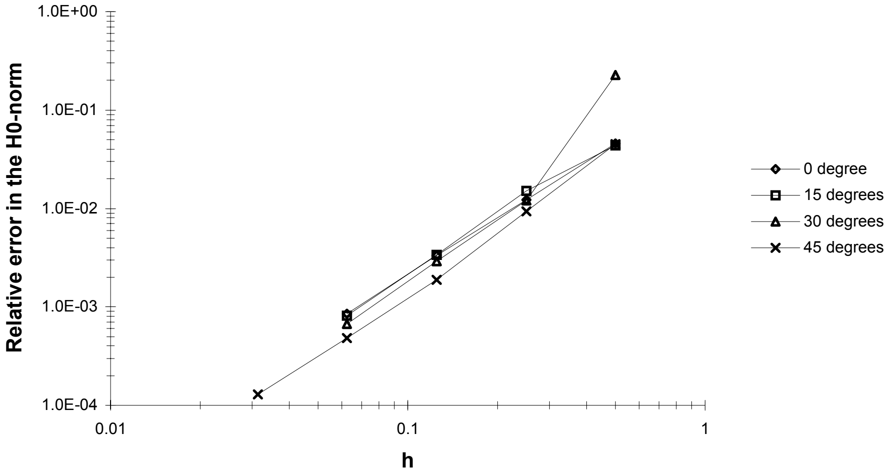

Figure 5. Relative error in the H_0-norm versus h for different orientation angles.

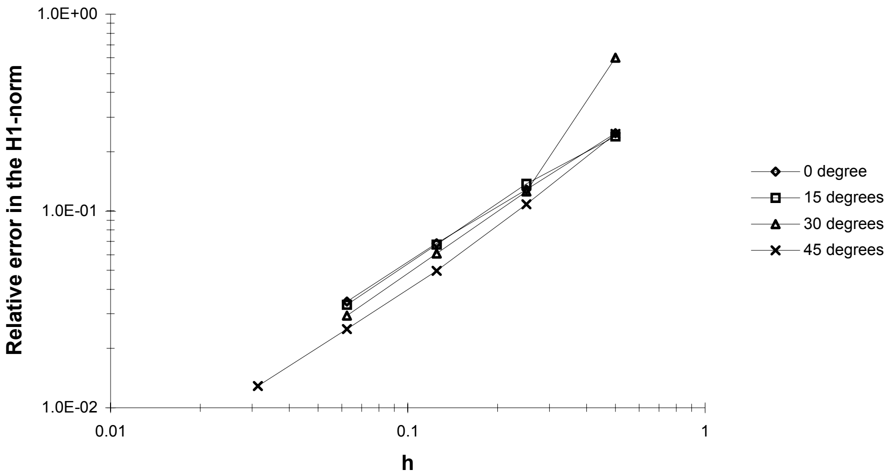

Figure 6. Relative error in the H_1-norm versus h for different orientation angles.

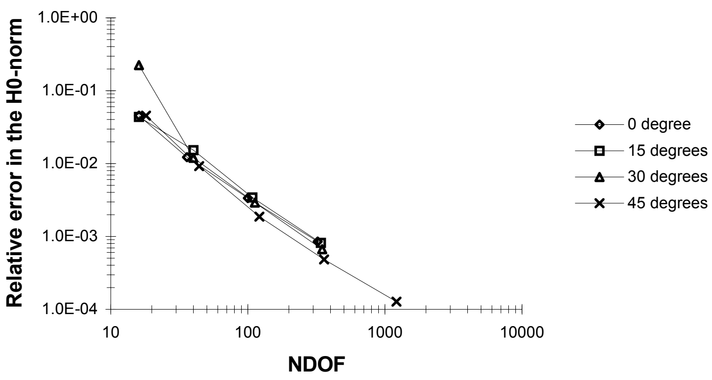

Figure 7. Relative error in the H_0-norm versus $NDOF$ for different orientation angles.

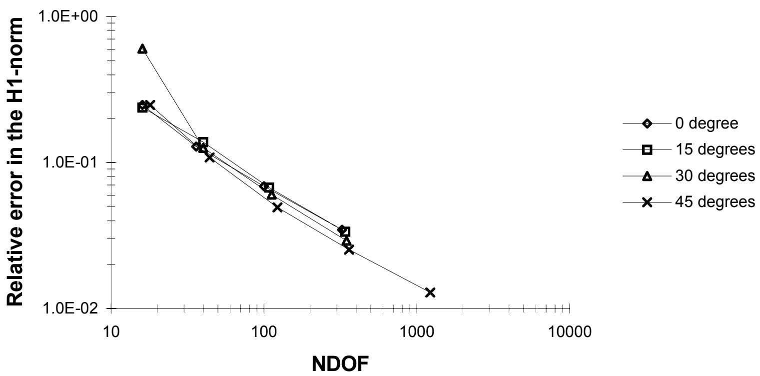

Figure 8. Relative error in the H_1-norm versus *NDOF* for different orientation angles.

As can be depicted from Figs. (5) and (6), the rates of convergence achieved are 2 and 1, respectively, in agreement to that expected for such problems, i. e., $O(h^{p+1-m})$, where p is the degree of the polynomial of the shape functions and m is order of the respective Hilbert space.

Figures (7) and (8) show the computational effort associated to a given solution precision. In the range of *NDOF* utilized it is observed that the number of degrees of freedom are increased approximately three times as the element size is halved.

4.2. Influence of the relative orientation of the mesh

Now, the influence of the relative orientation α on the relative error is investigated. For fixed element size h, α is ranged from 0^o to 45^o in increments of 15^o. Figure (9) shows the relative error in the H_0-norm, and Fig. (10) in the H_1-norm, versus the angle α for different element sizes h.

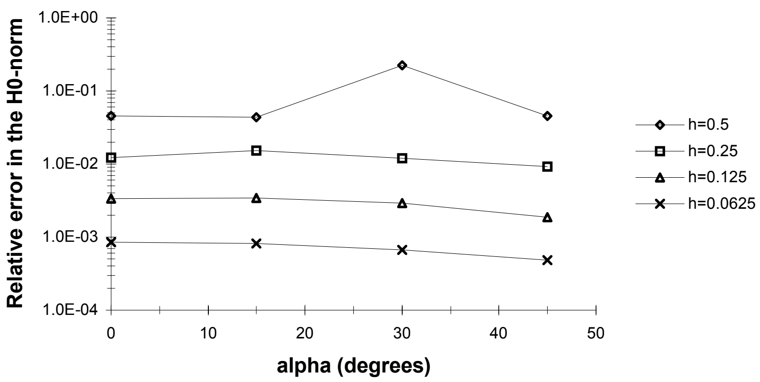

Figure 9. Relative error in the H_0-norm versus α for different h.

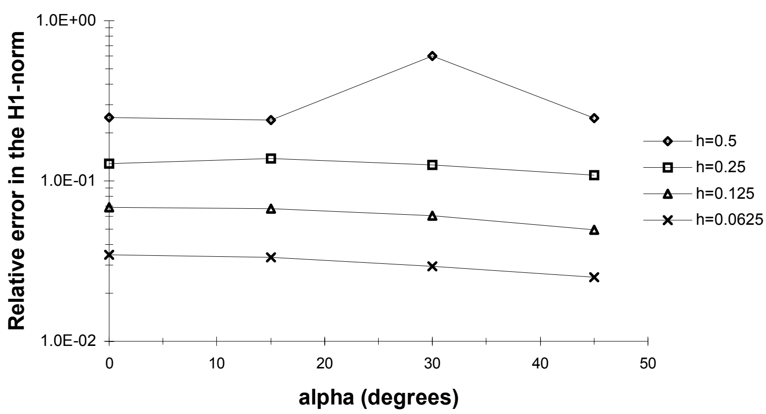

Figure 10. Relative error in the H_1-norm versus α for different h.

It is worth noting in Figs. (9) and (10) that no special trend is registered when the orientation angle is changed, suggesting that no special care is necessary regarding the orientation of the mesh.

5. Conclusions

The FEM was implemented and applied to a two-dimensional Poisson problem with a covering mesh of regular bilinear square elements. The numerical results obtained reveal the same performance as the standard FEM, and they also show that no especial care is needed respect to the orientation of the mesh relative to the domain.

The results obtained here are poorer than those obtained by the GFEM (Strouboulis et all, 2000 (1), 2000 (2) and 2001; Oden et all, 1998; Sukumar et all, 2000 and Duarte et all, 2000). The reason for this stems on the fact that the main advantage of the GFEM, i.e., base functions enrichment, was not implemented here, but only the covering, the orientation and the regularity of the mesh were examined. In the example run here, better results could be reached if the standard FEM base functions was enriched by bilinear polynomials, retrieving the exact solution, as can be depicted from *Theorem 1* of Oden et all (1998) and the quadratic form of Eq. (16). In this sense, this work complements the ones mentioned above, as the covering mesh, its orientation and its regularity are more explored here.

A simple manner to perform integrations was proposed where the boundary line intercepting the element was approximated as straight, considerably diminishing the quadrature effort on the contour elements. Furthermore, on the elements completely inside the domain, the integrations were given by a simple algebraic formula and consequently the computational time spent on them was minimum.

The imposition of boundary conditions through Lagrange multipliers technique is a source of solution instability (Strouboulis et all, 2000(1)) that should be object of further research on the application of a covering mesh in the FEM.

As a uniform refinement considerably increases the amount of degrees of freedom used, the implementation of local *h*-refinement to the regular mesh is strongly recommended for future research. The way suggested by Strouboulis et all (2000(1)) and Strouboulis et all (2001), where each square element is successively divided into 4 new equal square elements, seems to be a suitable alternative for maintaining the aspect ratio in a local *h*-refinement of the mesh. In this sense, a wide field to be explored is the enrichment of the base functions of finite elements by specific functions as proposed by the GFEM.

The method proposed can significantly simplify the mesh generation process, reducing costs in FEM numerical simulations, in training FEM customers and even diminishing the cost of a FEM package. Compared to the meshless methods, this has the indubitable advantage of several years of research on FEM and it is much easier to be implemented than the formers.

These few but significant results encourage further researches on this different approach of finite element.

6. References

Belytschko, T., Lu, Y.Y.; Gu, L., 1994, "Element-Free Galerkin Method", Int. J. Numer. Meth. Engng., Vol. 37, pp. 229-256.

Duarte, C. A., 1995, "A Review of Some Meshless Methods to Solve Partial Differential Equations", TICAM Report 95-6, 37 p.

Duarte, C. A., 1996, "The hp Cloud Method", Thesis, University of Texas at Austin, 215 p.

Duarte, C. A., Babuska, I., Oden, J. T., 2000, "Generalized finite element methods for three-dimensional structural mechanics problems", Computers and Structures, Vol. 77, pp. 215-232.

Duarte, C. A. and Oden, J. T., 1995, "Hp Clouds – A Meshless Method to Solve Boundary –Value Problems", TICAM Report 95-5, 65 p.

Melenk, J. M., Babuska, I., 1996, "The partition of unity finite element method: Basic theory and applications", Comput. Methods Appl. Mech. Engrg., Vol. 139, pp. 289-314.

Oden J. T., Duarte, C. A. M., Zienkiewicz, O. C., 1998, "A New cloud-based *hp* finite element method", Comput. Methods Appl. Mech. Engrg., Vol. 153, pp. 117-126.

Strouboulis, T., Babuska, I. and Copps, K., 2000(1), "The design and analysis of the Generalized Finite Element Method", Comput. Methods Appl. Mech. Engrg., Vol. 181, pp. 43-69.

Strouboulis, T., Copps, K. and Babuska, I., 2000(2), "The generalized finite element method: an example of its implementation end illustration of its performance", Int. J. Numer. Meth. Engng., Vol. 47, pp. 1401-1417.

Strouboulis, T., Copps, K. and Babuska, I., 2001, "The generalized finite element method", Comput. Methods Appl. Mech. Engrg., Vol. 190, pp. 4081-4193.

Sukumar, N., Moës, N., Moran, B., Belytschko, T., 2000, "Extended finite element method for three-dimensional crack modeling", Int. J. Numer. Meth. Engng., Vol. 48, pp. 1549-1570.